Publishing House
AKAPIT

COMPUTER METHODS IN MATERIALS SCIENCE

Informatyka w Technologii Materiałów

Vol. 9, 2009, No. 2

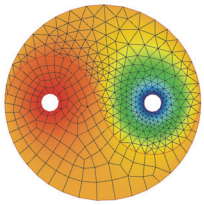

FINITE DIFFERENCE MODEL OF SHORT-PULSE LASER INTERACTIONS WITH THIN METAL FILM

EWA MAJCHRZAK[1], BOHDAN MOCHNACKI[2], JÓZEF S. SUCHY[3]

[1]Silesian University of Technology, Gliwice, Poland
[2]Czestochowa University of Technology, Czestochowa, Poland
[3]AGH, University of Science and Technology, Kraków, Poland
Corresponding Author: moch@imi.pcz.pl (B. Mochnacki)

Abstract

Thermal processes in a thin metal film subjected to a short-pulse laser heating are considered. The heat transfer proceeding in domain analyzed (microscale heat transfer) is described by means of the dual-phase-lag-model (DPLM) and the mathematical description of the process bases on the equation in which the relaxation time and thermalization time appear. The pulse laser action is taken into account by an additional term in energy equation corresponding to internal heat source, at the same time along the boundaries limiting a system the non-flux conditions are assumed. On a stage of numerical modelling a three level implicit finite difference scheme has been developed. A geometry of thin film allows to consider a 1D task, and then a solution of only one three-diagonal linear system of equations corresponds to transition from time t to t +Δt. In this place the Thomas algorithm has been used. In a final part of paper the examples of computations are shown.

Key words: microscale heat transfer, laser pulse, numerical simulation

1. INTRODUCTION

In the paper the mathematical model, numerical algorithm and examples of computations connected with the ultrafast heating of thin films are discussed. Heat transfer through thin films subjected to an ultrafast laser pulse is of vital importance in microtechnology applications and it is a reason that the problems connected with a fast heating of solids have become a very active research area.

The typical mathematical model of heat conduction basing on the Fourier equation is, in the case discussed, inadequate. It results from the fact that in reality the rate of thermal wave propagation is a finite one, and this phenomenon is essential when the time-rate change of temperature is high. So, the differences between the macroscopic heat conduction equation basing on the Fourier law and the models describing the ultrafast laser pulse interactions with metal films appear because of extremely short duration, extreme temperature gradients and geometrical features of domain considered [3,6,12, 13,14].

At present one can find the different models describing the mechanism of process discussed, below the microscopic two-step parabolic model will be applied [1,8]. The two-step parabolic model involves two energy equations determining the thermal processes in the electron gas and the metal lattice. As will be shown, it is also possible to transform this model to the equation containing a second order time derivative and higher order mixed derivative in both time and space. In the energy equation two characteristic parameters τ_q and τ_T appear. They

 ISSN 1641-8581

correspond to the relaxation time, which is the mean time for electrons to change their energy states and the thermalization time, which is the mean time required for electrons and lattice to reach equilibrium [11].

A two-step model involves two energy equations determining the heat exchange in the electron gas and the metal lattice. The equations creating the model discussed can be written in the form

$$c_e(T_e)\frac{\partial T_e}{\partial t} = \nabla\left[\lambda_e(T_e)\nabla T_e\right] - G(T_e - T_l) \quad (1)$$

$$c_l(T_l)\frac{\partial T_l}{\partial t} = \nabla\left[\lambda_l(T_l)\nabla T_l\right] + G(T_e - T_l) \quad (2)$$

where $T_e = T_e(x, t)$, $T_l = T_l(x, t)$ are the temperatures of electrons and lattice, respectively, $c_e(T_e)$, $c_l(T_l)$ are the volumetric specific heats, $\lambda_e(T_e)$, $\lambda_l(T_l)$ are the thermal conductivities, G is the coupling factor which characterizes the energy exchange between phonon and electrons [1] and is given as

$$G = \frac{\pi^4 (n_e v_s k)^2}{\lambda_e} \quad (3)$$

at the same time

$$v_s = \frac{k}{2\pi h}\left(6\pi^2 n_a\right)^{-1/3} \quad (4)$$

where n_e is the volumetric electron number density, n_a is the volumetric atomic density, k is the Boltzmann constant, h is the Planck constant, v_s is the speed of sound.

In the case of pure metals the system of equations (1) and (2) under the assumption that volumetric specific heats c_e and c_l are the constant values can be simplified to the form

$$c_e\frac{\partial T_e}{\partial t} = \nabla(\lambda_e \nabla T_e) - G(T_e - T_l) \quad (5)$$

$$c_l\frac{\partial T_l}{\partial t} = G(T_e - T_l) \quad (6)$$

This simplification, according to [1], results from the fact that the incident radiation and conductional heat flux are absorbed and diffused mainly by electrons.

The equations (5) and (6) using a simple mathematical technique can be substituted by a single equation containing a higher-order mixed derivative in both time and space [4,5]. Using the equation (6) one has

$$T_e = T_l + \frac{c_l}{G}\frac{\partial T_l}{\partial t} \quad (7)$$

Putting (7) into (5) the following form of energy equation can be found

$$c_e\left(\frac{\partial T_l}{\partial t} + \frac{c_l}{G}\frac{\partial^2 T_l}{\partial t^2}\right) = \nabla(\lambda_e \nabla T_l) + \frac{c_l}{G}\nabla\left[\lambda_e \frac{\partial}{\partial t}(\nabla T_l)\right] - c_l\frac{\partial T_l}{\partial t} \quad (8)$$

this means

$$(c_e + c_l)\frac{\partial T_l}{\partial t} + \frac{c_e c_l}{G}\frac{\partial^2 T_l}{\partial t^2} = \nabla(\lambda_e \nabla T_l) + \frac{c_l}{G}\frac{\partial}{\partial t}\left[\nabla(\lambda_e \nabla T_l)\right] \quad (9)$$

or

$$(c_e + c_l)\left[\frac{\partial T_l}{\partial t} + \frac{c_e c_l}{G(c_e + c_l)}\frac{\partial^2 T_l}{\partial t^2}\right] = \nabla(\lambda_e \nabla T_l) + \frac{c_l}{G}\frac{\partial}{\partial t}\left[\nabla\lambda_e(\nabla T_l)\right] \quad (10)$$

Denoting

$$\tau_T = \frac{c_l}{G}, \quad \tau_q = \frac{1}{G}\left(\frac{1}{c_e} + \frac{1}{c_l}\right)^{-1} \quad (11)$$

finally one obtains

$$c\left(\frac{\partial T(x, t)}{\partial t} + \tau_q \frac{\partial^2 T(x, t)}{\partial t^2}\right) = \nabla\left[\lambda \nabla T(x, t)\right] + \tau_T \nabla\left[\lambda \frac{\partial \nabla T(x, t)}{\partial t}\right] \quad (12)$$

where $T(x, t) = T_l(x, t)$ is the macroscopic lattice temperature [12], $c = c_l + c_e$ is the effective volumetric specific heat resulting from the serial assembly of electrons and phonons and $\lambda = \lambda_e$ [16]. As was mentioned, the positive constants τ_q and τ_T correspond to relaxation time and thermalization time, respectively, and they are characteristic for the so-called dual-phase-lag model.

The laser-film interaction is taken into account by use of internal volumetric heat source appearing in the microscopic heat transfer equation. In this

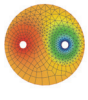

paper the following formula [7,15] determining the capacity of internal heat sources has been applied

$$Q(x,t)=\sqrt{\frac{\beta}{\pi}}\,\frac{1-R}{t_p\,\delta}I_0\exp\left[-\frac{x}{\delta}-\beta\frac{(t-2t_p)^2}{t_p^2}\right] \quad (13)$$

where I_0 is the laser intensity which is defined as the total energy carried by a laser pulse per unit cross-section of the laser beam, t_p is the characteristic time of laser pulse, δ is the characteristic transparent length of irradiated photons called the absorption depth, R is the reflectivity of the irradiated surface and $\beta = 4\ln 2$ [2]. The local and temporary value of Q results from the distance x between surface subjected to laser action and the point considered.

The presence of internal heat sources $Q(x, t)$ in domain considered, leads to the more complex form of equation (12), namely

$$c\left(\frac{\partial T(x,t)}{\partial t}+\tau_q\frac{\partial^2 T(x,t)}{\partial t^2}\right)=\nabla\left[\lambda\nabla T(x,t)\right]+\tau_T\nabla\left[\lambda\frac{\partial\nabla T(x,t)}{\partial t}\right]+Q(x,t)+\tau_q\frac{\partial Q(x,t)}{\partial t} \quad (14)$$

In a case of laser pulse interactions with thin films, the laser spot size is much larger than film thickness, additionally the film thickness is essentially less than the remaining dimensions. Therefore, it is reasonable to treat the interactions as a one-dimensional heat transfer process [2] and then the following energy equation should be considered

$$c\left(\frac{\partial T(x,t)}{\partial t}+\tau_q\frac{\partial^2 T(x,t)}{\partial t^2}\right)=\frac{\partial}{\partial x}\left[\lambda\frac{\partial T(x,t)}{\partial x}\right]+\tau_T\frac{\partial}{\partial x}\left[\lambda\frac{\partial^2 T(x,t)}{\partial x\,\partial t}\right]+Q(x,t)+\tau_q\frac{\partial Q(x,t)}{\partial t} \quad (15)$$

The initial condition supplementing the equation (15) determines the initial temperature distribution $T(x, 0) = T_0$ and initial heating rate $\partial T(x, 0)/\partial t = 0$, while the boundary conditions for $x = 0$ and $x = L$ correspond to the non-flux ones.

2. NUMERICAL MODEL

On the stage of numerical computations the finite difference method has been used. The differential mesh is a cartesian product of spatial Δ_h and time Δ_t meshes. Time grid is defined as follows

$$\Delta_t:\quad t^0<t^1<\ldots<t^{f-2}<t^{f-1}<t^f<\ldots<t^F<\infty \quad (16)$$

while the spatial mesh is shown in Figure 1.

It is visible that the 'boundary' nodes are located at the distance $0.5h$ from real boundaries (this type of discretization assures a very simple and exact approximation of boundary conditions [10]).

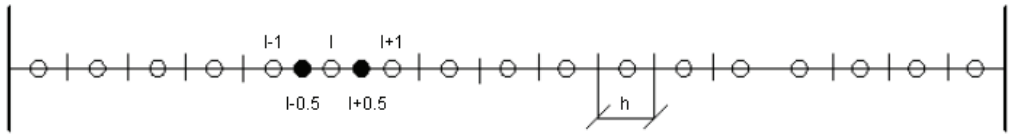

Fig. 1. *The mesh.*

It can be shown that FDM approximation of spatial differential operator can be taken in the form [10]

$$\frac{\partial}{\partial x}\left(\lambda\frac{\partial T}{\partial x}\right)_i^f=\frac{T_{i+1}^f-T_i^f}{R_{i+1}^{f-1}}\Psi_{i+1}+\frac{T_{i-1}^f-T_i^f}{R_{i-1}^{f-1}}\Psi_{i-1} \quad (17)$$

where $\Psi_{i+1}=\Psi_{i-1}=1/h$, while

$$R_{i+1}^{f-1}=\frac{0.5h}{\lambda_i^{f-1}}+\frac{0.5h}{\lambda_{i+1}^{f-1}},\quad R_{i-1}^{f-1}=\frac{0.5h}{\lambda_i^{f-1}}+\frac{0.5h}{\lambda_{i-1}^{f-1}} \quad (18)$$

are the thermal resistances between node i and adjoining nodes $i + 1$, $i - 1$.

An index f in formula (17) shows that the implicit differential scheme will be used here, at the same time, the thermal conductivities are taken for time t^{f-1} to obtain the linear form of final FDM equations.

The FDM approximation of equation (15) for transition $t^{f-1}\rightarrow t^f$ is of the form

$$c\frac{T_i^f-T_i^{f-1}}{\Delta t}+c\tau_q\frac{T_i^f-2T_i^{f-1}+T_i^{f-2}}{(\Delta t)^2}=\frac{T_{i+1}^f-T_i^f}{R_{i+1}^{f-1}}\Psi_{i+1}+\frac{T_{i-1}^f-T_i^f}{R_{i-1}^{f-1}}\Psi_{i-1}+\frac{\tau_T}{\Delta t}\left(\frac{T_{i+1}^f-T_i^f}{R_{i+1}^{f-1}}\Psi_{i+1}+\frac{T_{i-1}^f-T_i^f}{R_{i-1}^{f-1}}\Psi_{i-1}\right)-$$

$$\frac{\tau_T}{\Delta t}\left(\frac{T_{i+1}^{f-1}-T_i^{f-1}}{R_{i+1}^{f-1}}\Psi_{i+1}+\frac{T_{i-1}^{f-1}-T_i^{f-1}}{R_{i-1}^{f-1}}\Psi_{i-1}\right)+ \quad (19)$$

$$Q_i^f+\tau_q\left(\frac{\partial Q}{\partial t}\right)_i^f$$

and the last equation can be written as follows

$$A_i T_{i-1}^f + B_i T_i^f + C_i T_{i+1}^f =$$

$$D_i T_{i-1}^{f-1} + E_i T_i^{f-1} + F_i T_{i+1}^{f-1} + \frac{\tau_q}{(\Delta t)^2} T_i^{f-2} -$$

$$\frac{Q_i^f}{c} - \frac{\tau_q}{c}\left(\frac{\partial Q}{\partial t}\right)_i^f, \quad i=1, 2, ..., N \quad (20)$$

where

$$A_i = \frac{\Psi_{i-1}}{c\,R_{i-1}^{f-1}}\left(1+\frac{\tau_T}{\Delta t}\right), \qquad C_i = \frac{\Psi_{i+1}}{c\,R_{i+1}^{f-1}}\left(1+\frac{\tau_T}{\Delta t}\right) \quad (21)$$

$$B_i = -\frac{1}{\Delta t}\left(1+\frac{\tau_q}{\Delta t}\right) - A_i - C_i \quad (22)$$

$$D_i = \frac{\Psi_{i-1}}{c\,R_{i-1}^{f-1}}\frac{\tau_T}{\Delta t}, \qquad F_i = \frac{\Psi_{i+1}}{c\,R_{i+1}^{f-1}}\frac{\tau_T}{\Delta t} \quad (23)$$

$$E_i = -\frac{1}{\Delta t}\left(1+\frac{2\tau_q}{\Delta t}\right) - D_i - F_i \quad (24)$$

Finally

$$A_i T_{i-1}^f + B_i T_i^f + C_i T_{i+1}^f = G_i^f \quad (25)$$

where

$$G_i^f = D_i T_{i-1}^{f-1} + E_i T_i^{f-1} + F_i T_{i+1}^{f-1} +$$

$$\frac{\tau_q}{(\Delta t)^2} T_i^{f-2} - \frac{Q_i^f}{c} - \frac{\tau_q}{c}\left(\frac{\partial Q}{\partial t}\right)_i^f \quad (26)$$

The same equations are accepted for the nodes close to boundaries. It is enough to assume that the thermal resistances in directions 'to boundary' are sufficiently big (e.g. 10^{10}) and then the non-flux condition is taken into account. The start point of numerical simulation process results from the initial conditions, in particular $T_i^0 = T_i^1 = T_0$, $i=1, 2, ... N$. As was mentioned, the system of FDM equations (25) has been solved using the Thomas algorithm [9] for three-diagonal linear system.

3. EXAMPLES OF COMPUTATIONS

The thin film of thickness $L = 200$ nm (1 nm = 10^{-9} m) is considered (gold, chromium). The layer is subjected to a short-pulse laser irradiation which parameters are equal to: $R = 0.93$ (reflectivity), I_0=13.7 J/m^2 (intensity), t_p = 0.1 ps = 10^{-13} s (time of laser pulse), δ = 15.3 nm (absorption depth).

The following parameters of gold thin film are assumed: thermal conductivity λ = 317 W/(mK), volumetric specific heat c = 2.4897 MJ/(m^{3}K), relaxation time τ_q = 8.5 ps, thermalization time τ_T = 90 ps [4,5]. Initial temperature equals T_0 = 20 ^{o} C. Using the algorithm presented in the previous chapter under the assumption that N = 200 (h=1 nm) and Δt = 0.005 ps the transient temperature field has been found. In figure 2 the temperature profiles are shown, while figure 3 illustrates the courses of heating (cooling) curves at the points selected from the domain considered.

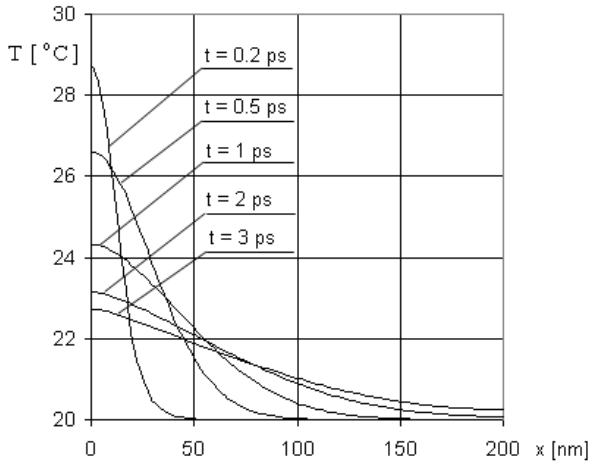

Fig. 2. *Temperature profiles for different times(gold film).*

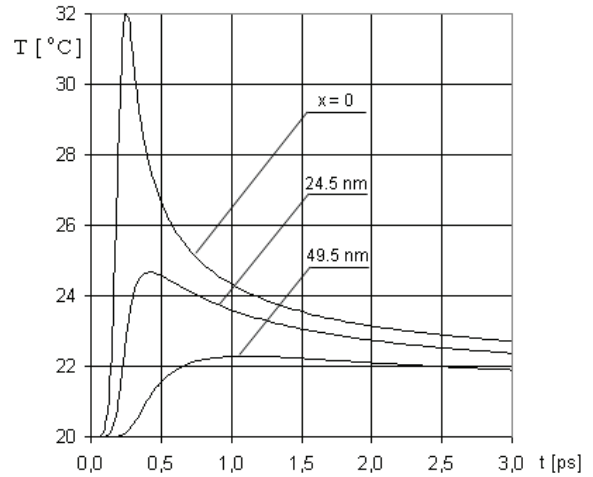

Fig. 3. *Cooling (heating) curves at the points from gold film domain.*

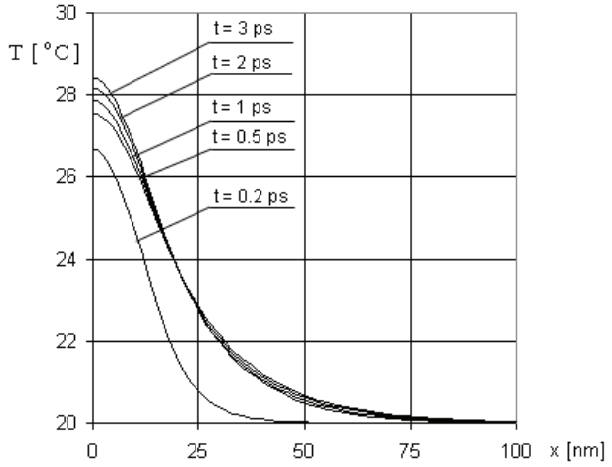

Fig. 4. *Temperature profiles for different times (chromium film).*

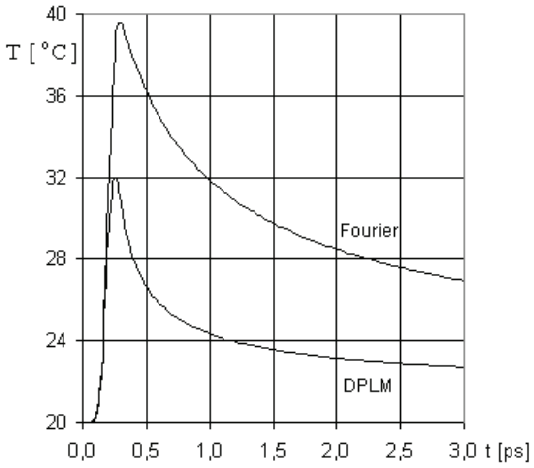

Fig. 6. *Comparison of models – gold.*

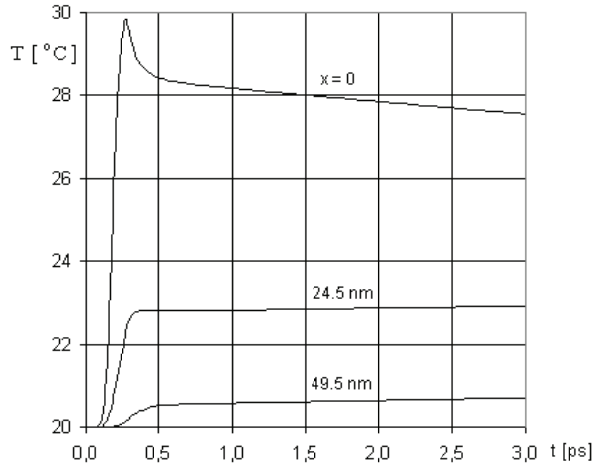

Fig. 5. *Cooling (heating) curves at the points from chromium film domain.*

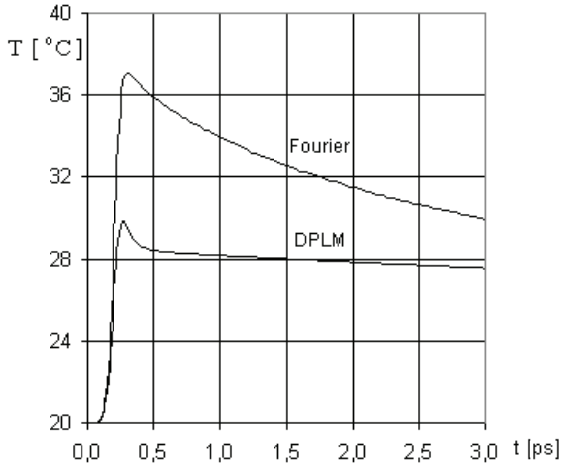

Fig. 7. *Comparison of models – chromium.*

The computations are also done for the chromium thin film (figures 4 and 5) under the assumption that $\lambda = 93$ W/(mK), $c = 3.21484$ MJ/(m^3 K), $\tau_q = 0.136$ ps and $\tau_T = 7.86$ ps [4, 5].

In figures 6 and 7 the comparisons of temperature courses for gold and chromium thin layers at the surface subjected to a laser pulse obtained by means of the dual-phase-lag-model (DPLM) and the Fourier one are shown.

The solutions found for different materials are different, of course. One can notice the similarities only from a qualitative view-point. Both solutions essentially differ in courses from solutions corresponding to the Fourier equation. The authors had not the possibilities of direct verification of results, but it should be pointed out that algorithm proposed has been tested using the analytical solution of simplified model (benchmark) quoted in [5] and the results have been practically the same.

The algorithm presented can be simply generalized on the cases of 2D or 3D tasks, but on a stage of computations the problems connected with a very big number of nodes and a short time interval can appear.

ACKNOWLEDGEMENT

The paper is a part of project MTKD-CT-2006-042468.

REFERENCES

1. Al-Nimr, M.A., Heat transfer mechanisms during short duration laser heating of thin metal films, Int. J. of Thermophysics, 18, 5, 1997, 1257-1268.
2. Chen, J.K., Beraun, J.E., Numerical study of ultrashort laser pulse interactions with metal films, Numerical Heat Transfer, Part A, 40, 2001, 1-20.
3. Chen, G., Borca-Tasciuc, D., Yang, R.G., Nanoscale heat transfer, Encyclopedia of Nanoscience and Nanotechnology, Edited by H.S.Nalwa, Volume X, 2004, 1-30.
4. Dai, W., Nassar, R., A domain decomposition method for solving three-dimensional heat transport equations in

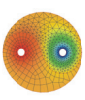

a double-layered thin film with microscale thickness, Numerical Heat Transfer, Part A, 38, 2000, 243-255.
5. Dai, W., Nassar, R., A compact FD scheme for solving a one-dimensional heat transport equation at the microscale, J. of Comp. and Appl. Math., 132, 2001, 431-441.
6. Escobar, R.A., Ghau, S.S., Jhon, M.S., Amon, C.H., Multi-length and time scale thermal transport using the lattice Boltzmann method with application to electronic cooling, International J. of Heat and Mass Transfer, 49, 2006, 97-107.
7. Kaba, I.K., Dai, W., A stable three-level finite difference scheme for solving the parabolic two- step model in a 3D micro-sphere heated by ultrashort-pulsed lasers, J. of Computational and Applied Mathematics, 181, 2005, 125-147.
8. Lin, Z., Zhigilei, L.V., Electron-phonon coupling and electron heat capacity of metals under conditions of strong electron-phonon nonequilibrium, Physical Review, B 77, 2008, 075133-1-075133-17.
9. Majchrzak, E., Mochnacki, B., Metody numeryczne. Podstawy teoretyczne, aspekty praktyczne i algorytmy. Wyd. Pol. Śl. Gliwice, 2004.
10. Mochnacki, B., Suchy J.S., Numerical methods in computations of foundry processes, Polish Foundrymen's Technical Association, Kraków, 1995.
11. Orlande, H.R.B., Özişik, M.N., Inverse analysis for estimating the electron-phonon coupling factor in thin metal films, J. of Applied Physics, 78 (3), 1995, 1843-1849.
12. Özişik, M.N., Tzou, D.Y., On the wave theory in heat conduction, J. of Heat Transfer, 116, 1994, 526-535.
13. Smith, A.N., Norris, P.M., Microscale heat transfer, Heat Transfer Handbook, John Wiley & Sons, 2003.
14. Tamma, K.K., Zhou, X., Macroscale and microscale thermal transport and thermo-mechanical interactions: some noteworthy perspectives, Journal of Thermal Stresses, 1998, 405-449.
15. Tang, D.W., Araki, N., Wavy, wavelike, diffusive thermal responses of finite rigid slabs to high-speed heating of laser-pulses, Int. J. of Heat and Mass Transfer, 42, 1999, 855-860.
16. Tzou, D.Y., Chiu, K.S., Temperature-dependent thermal lagging in ultrafast laser heating, Int. J. of Heat and Mass Transfer, 44, 2001, 1725-1734.

MODEL RÓŻNICOWY ODDZIAŁYWAŃ TERMICZNYCH LASERA O KRÓTKIM IMPULSIE NA WARSTEWKĘ METALOWĄ

Streszczenie

Rozważano procesy cieplne zachodzące w cienkiej warstewce metalowej poddanej działaniu lasera o krótkim impulsie. Przepływ ciepła w analizowanym obszarze (w skali mikro) opisuje model podwójnego opóźnienia i opis matematyczny procesu bazuje na równaniu, w którym pojawia się czas relaksacji oraz czas termalizacji. Oddziaływanie lasera uwzględniono w dodatkowym składniku równania energii odpowiadającym wewnętrznej funkcji źródła, równocześnie na powierzchniach ograniczających założono warunki adiabatyczne. Na etapie modelowania numerycznego opracowano trójpoziomowy niejawny schemat metody różnic skończonych. Biorąc pod uwagę geometrię cienkiej warstewki, rozpatrywano zadanie 1D (jednowymiarowe) i wówczas dla każdego przejścia od chwili t do chwili $t + \Delta t$ należy rozwiązać tylko jeden trójdiagonalny układ równań. Układ ten rozwiązano wykorzystując algorytm Thomasa. W końcowej części artykułu pokazano przykłady obliczeń.

Submitted: September 25, 2008
Submitted in a revised form: October 19, 2008
Accepted: October 30, 2008